PHYSICAL REVIEW B

CONDENSED MATTER

THIRD SERIES, VOLUME 52, NUMBER 13 1 OCTOBER 1995-I

BRIEF REPORTS

Brief Reports are accounts of completed research which, while meeting the usual **Physical Review B** *standards of scientific quality, do not warrant regular articles. A Brief Report may be no longer than four printed pages and must be accompanied by an abstract. The same publication schedule as for regular articles is followed, and page proofs are sent to authors.*

Crystal grain growth during phase transformation in cerium metal at high pressure

Guoliang Gu and Yogesh K. Vohra

Department of Physics, University of Alabama at Birmingham, Birmingham, Alabama 35294-1170

Keith E. Brister

Cornell High Energy Synchrotron Source, Cornell University, Ithaca, New York 14853

(Received 9 May 1995)

Crystal structures and orientation effects in cerium (Ce) metal were investigated in the pressure range of 0–28 GPa by high-resolution synchrotron x-ray diffraction using image plate technique with a diamond-anvil cell. We observe crystal grain growth during the phase transformations to α-uranium structure both during compression and decompression cycle. We offer explanation for the long-standing controversy on the intermediate phases and attribute various crystal structure proposals to low-resolution and orientation effects. This crystal grain growth during phase transformation in Ce at high pressure and ambient temperature is an unusual phenomenon among metals.

The f-electron metals have been the focus of intense experimental and theoretical high-pressure research in the last several decades.[1–5] This is largely due to the unique behavior of f-electrons under pressure and their delocalization and participation in bonding. Cerium (Ce) is a classic example of an electronic transition with one localized electron in the f shell. At ambient pressure and room temperature, Ce is normally obtained in the γ(fcc) phase. At room temperature, a volume collapse of about 16% is observed in 0.7 GPa in Ce.[4] This volume collapse is generally attributed to a dramatic change in f-electron character from a localized shell to a state interacting with spd conduction electrons and other f electrons.[2,5] Above 13 GPa, Ce is known to be in the body-centered-tetragonal (bct) structure.[7] This bct phase is stable to ultrahigh pressures in Ce, thorium, and their alloys.[7–10] Even though cerium has been extensively studied in the last several decades, there is no consensus regarding the crystal structure in the 5–13 GPa range. There have been several proposals of the stable crystal structures such as the α-uranium structure (α' phase) by Zachariasen and Ellinger[6] and the body-centered-monoclinic (bcm) structure (α'' phase) by Olsen *et al.*[8] We notice that the early x-ray-diffraction studies were limited by two factors: (1) low resolution of the energy dispersive technique usually employed in this work and (2) orientation effects as first documented by Zachariasen and Ellinger.[6] In recent years, a high-resolution image plate technique has been introduced in high-pressure research.[11,12] The high resolution and wide dynamic range of the image plate technique provide a very powerful tool to record both strong peaks and weak peaks in the x-ray-diffraction spectrum. These virtues are very critical in the studies of low-symmetry structures encountered in rare-earth metals after f delocalization. In this paper we report a very interesting phenomenon of crystal grain growth during phase transformation at room temperature and high pressure that is specific to Ce metal. We also clarify some of the long-standing issues in crystal structure of Ce at high pressure.

Two separate high-pressure experiments were carried out on Ce metal. The first experiment was carried out on Ce without a pressure standard with the goal of obtaining diffraction patterns with the least extraneous lines. The second experiment on Ce included a copper pressure standard for *in-situ* pressure measurement. The experiments were carried out with diamond anvils 600 μm in diameter. The Ce sample ($\sim$100 μm in diameter) cut from a high-purity (99.99%) ingot was loaded into a hole 150 μm in diameter. The mixture of methanol:ethanol was employed to provide the quasihydrostatic environment for the Ce sample. The experiments were carried

out on the D line at the Cornell High Energy Synchrotron Source (CHESS). The monochromotized incident x-ray beam ($\lambda=0.4066$ Å) passes through the 100 μm$\times$100 μm collimator. The sample-film distance of 274.51 mm is determined from the diffraction pattern of Ce at ambient pressure and the literature value of the Ce lattice parameter ($a=5.1608$ Å). The exposed Fuji high-resolution image plate (HR-IIIN 20.1 cm$\times$25.2 cm) was processed by a FUJIX BAS 2000 scanner. The pixel size is 100 μm $\times$100 μm. The transmitted x-ray beam was attenuated by a lead block in order to keep the direct beam count below saturation level within a typical exposure time (30 min). This direct beam location on the film is an important parameter for cell parameter determination. The pressure calibration in the present experiments is based on the modified universal equation of state (MUEOS) given by Vinet *et al.*[13] with $B_0=143.7$ GPa, $B_0'=3.904$, and $\beta=13.77$ fitted to the shock-wave data of copper up to 240 GPa.[14] In the pressure range up to 30 GPa, the MUEOS for copper is in good agreement with the available ultrasonic equation of state[15,16] for copper. The differences between these two equations of state are only 0.3 GPa at 10 GPa and about 1 GPa at 30 GPa. We neglect these small differences in pressure obtained from various equations of state.

The Ce metal shows a well-documented collapse of 16% during the $\gamma\rightarrow\alpha$ phase transformation at 0.7 GPa. Below 5 GPa, all the diffraction images show clear fcc structures (γ or α) [Fig. 1(a)]. The diffraction rings are all continuous and uniform in intensity. These characteristics indicate the random orientation of the crystal planes. At 5 GPa, the Ce metal undergoes another structural phase transformation. Only a few strong diffraction spots and very weak α(fcc) diffraction rings are observed on the diffraction image [Fig. 1(b)]. This diffraction image indicates that considerable crystal grain growth has occurred during the phase transformation. It should be added that a conventional energy-dispersive x-ray-diffraction technique that employs point slit geometry will only detect crystalline phases with continuous rings.[8] The occurrence of only a few diffraction spots is a clear indication of crystal grain growth. On increasing pressure beyond 5 GPa, it leads to the breakup of large crystals into small polycrystals. This phenomenon is clear in Fig. 1(c), where continuous rings begin to form at 6 GPa. This tendency to form continuous rings continues till 13 GPa; above this pressure a discontinuous transformation to the bct phase is observed.[7]

The Debye-Scherrer rings were divided to eight sectors for radial intensity integration. After integrating the intensities for each sector, we get the diffraction pattern for intensity versus the distance from the beam center. This is then converted to the intensity-versus-2θ plot (Fig. 2) using the known sample-film distance. In Fig. 2, the intensity-versus-2θ plot shows the $\alpha'(\alpha$-U)-to-bct phase transformation around 13 GPa. Between 5 and 13 GPa the sample is in the $\alpha'(\alpha$-U) phase [Fig. 2(a)]. At 13 GPa, the bct phase emerges and coexists with the $\alpha'(\alpha$-U) phase [Fig. 2(b)]. The single-phase bct pattern was observed at a higher pressure of 19 GPa [Fig. 2(c)].

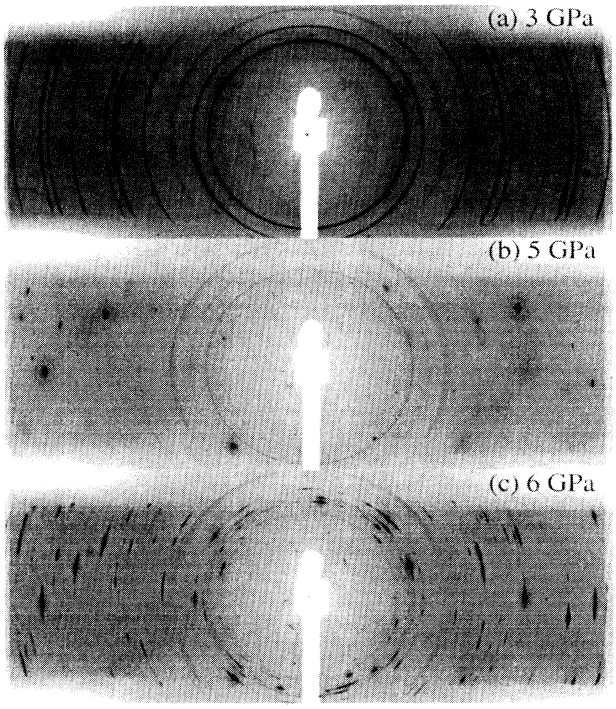

FIG. 1. X-ray-diffraction images of pure Ce metal at 3 GPa, 5 GPa, and 6 GPa, respectively. (a) At 3 GPa, the sample is in the fcc phase. (b) At 5 GPa, the large grain size of the α-U phase is indicated by only a few diffraction spots. The weak ring patterns are from the residual fcc phase. (c) The orientation effects decrease gradually at higher pressure, and rings tend to become continuous.

We tried to fit all the patterns obtained between 5 and 13 GPa as a $\alpha'(\alpha$-U) structure or a α''(bcm) structure as proposed the literature. Below 7 GPa, all of the diffraction peaks can be fitted as a phase mixture of α''(bcm) and $\alpha'(\alpha$-U) structures. At 6.9 GPa, the lattice parameters are $a=3.135$ Å, $b=3.173$ Å, $c=4.798$ Å, and $\beta=91.92°$ for the α''(bcm) structure and $a=3.047$ Å, $b=5.948$ Å, and $c=5.174$ Å for the $\alpha'(\alpha$-U) structures. The details of the structure fitting at 6.9 GPa are shown in Table I. The fact that the sample is a phase mixture is attributed to the occurrence of characteristic diffraction peaks of both phases. Above 7 GPa, the characteristic peaks for the α''(bcm) structure disappeared, and its structure fitting became worse as pressure increased. In contrast, the α-U structure can be fitted to most of the diffraction peaks. The only peak that cannot be fitted in the $\alpha'(\alpha$-U) structure is the peak close to α(fcc)(200) ($d=2.216$ Å at 8 GPa). This peak appeared after the transformation and can be explained as the diffraction peak from the superlattice of the α-U structure by doubling the unit cell along the **a** direction.

The highest pressure in our experiments is 28 GPa, and the crystal structure of the Ce sample under these conditions is bct [Fig. 3(a)]. During the decompression, the sample underwent a similar but reversed sequence of phase transformations as in the compression. The crystal grain growth was again observed when the sample trans-

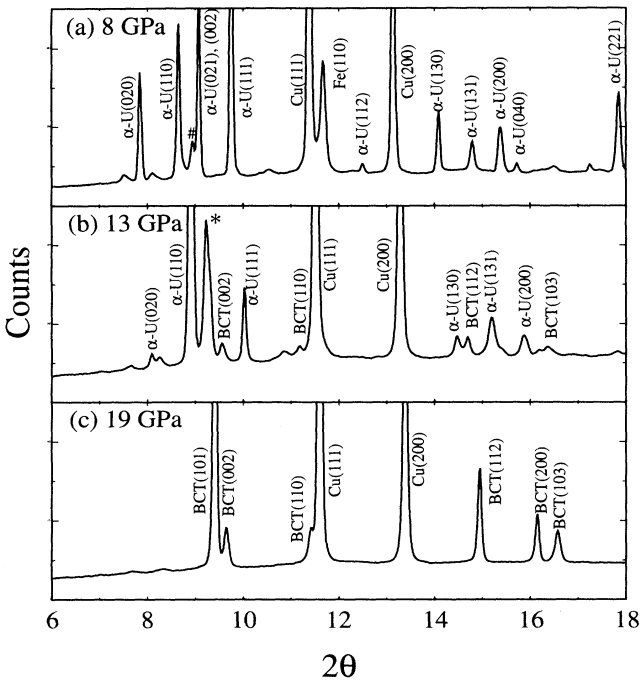

FIG. 2. The radially integrated diffraction patterns of the Ce with $\lambda=0.4066$ Å. (a) At 8 GPa the pattern is fitted to the α-U structure [the peak with the # label is from residual fcc(111)]. (b) At 13 GPa the bct phase emerges and coexists with the α-U phase [the peak with the * label is the mixture of α-U(021), (002), and bct(101)]. (c) The single phase bct diffraction pattern is shown at 19 GPa.

forms to the $\alpha'(\alpha$-U) phase [Fig. 3(b)]. A polycrystalline diffraction pattern was obtained when the sample became of fcc structure during the decompression cycle [Fig. 3(c)]. The crystal structure data from the present experiments is summarized in Fig. 4. The measured axial ratio for the $\alpha'(\alpha$-U) is relatively insensitive to the pressures. The axial c/a ratio for the bct phase increases with pressure and then tends to saturate to a value of 1.69 above 25 GPa. This trend in c/a ratio for the bct phase is consistent with the data on Th and Ce-Th alloys.[9,10]

It should be added that the phenomenon of crystal grain growth is different from the pressure-induced orientation effects (or texture) generally observed in metals under high pressure. It is now well-established that certain hexagonal close-packed metals develop a basal plane texture as a result of compression in the diamond-anvil cell device. This is manifested by the loss of (002) reflection in diffraction patterns of many hexagonal metals. In this situation of texture induced by plastic deformation, only certain diffraction rings become spotty, while others remain continuous.[17] However, in our case, we observe only a few diffraction spots on the entire image plate. The phenomenon we see is reminiscent of the crystal grain growth observed during recrystalization of cold worked metals at high temperature. However, what makes this phenomenon unique is that we observe this phenomenon at room temperature and high pressure in Ce metal. Similar image plate measurements were also carried out on the $Ce_{0.76}Th_{0.24}$ alloy up to 20 GPa.[17] In this Ce-Th alloy, neither the α(fcc)-to-α-U transformation nor the crystal grain growth was observed. This indicates that the

TABLE I. Image plate diffraction data at 6.9 GPa. All the observed peaks can be assigned to the phase mixture of $\alpha'(\alpha$-U), α''(bcm), and α(fcc) of Ce and the fcc phase of the copper pressure standard.

	hkl			
	Ce	Ce		
	$\alpha'(\alpha$-U) structure	α''(bcm) structure	Ce	Copper
	$a=3.047$, $b=5.948$	$a=3.135$, $b=3.173$	α(fcc) structure	fcc structure
d (Å)	$c=5.174$	$c=4.798$, $\beta=91.92°$	$a=4.538$	$a=3.561$
2.970	020			
2.665		10-1		
2.620			111	
2.584	021	101		
2.398	111	00-2		
2.264			200	
2.228		110		
2.054				111
1.872	112			
1.780				200
1.665	130			
1.650		11-2		
1.610		112	220	
1.586	131	020		
1.574		200		
1.522	200			
1.493	023			
1.465	201			
1.438	113	10-3		
1.434	041	01-3		
1.418	211			

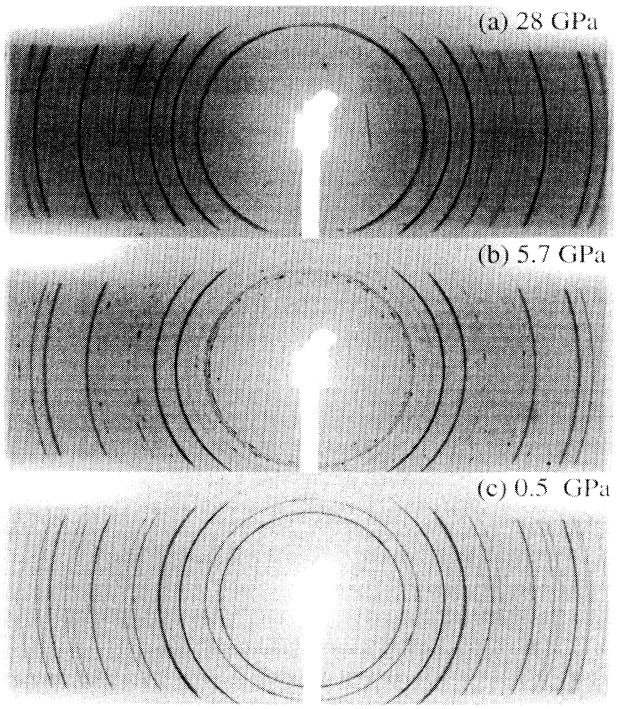

FIG. 3. X-ray-diffraction images of Ce metal mixed with the Cu pressure standard during decompression. (a) The diffraction rings are continuous and uniform in intensity for the bct phase at 28 GPa. (b) The spotty rings show the orientation effects in the α-U phase. (c) The rings become continuous and uniform again during back transformation to the fcc phase. Note that the Cu diffraction rings are always continuous through the decompression cycle.

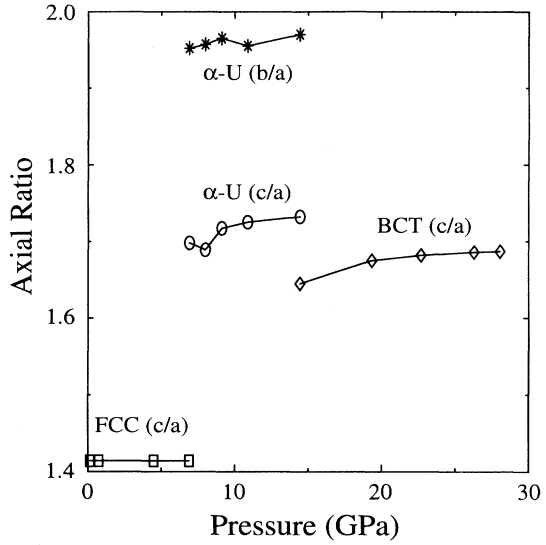

FIG. 4. The axial ratio of the various phases as a function of pressure in Ce. The fcc phase data are shown with a constant value of $c/a = 1.414$. The axial ratios for the α-U phase are relatively insensitive to pressure. The c/a ratio for the bct phase increases with pressure and tends to saturate at high pressure.

crystal grain growth observed in Ce metal is specific to the α(fcc)–to–α-U transformation only.

We offer the following conclusions.

(1) Crystal grain growth was observed in the formation of the $\alpha'(\alpha$-U) phase during both compression and the decompression cycles in Ce metal. This is a report for the pressure-induced crystal grain growth in metallic systems.

(2) Contrary to earlier suggestions,[8] our high-resolution x-ray-diffraction pattern supports the original suggestion of Zachariasen that the $\alpha'(\alpha$-U) phase is the stable phase of Ce between 5 and 13 GPa. The stability field of the α''(bcm) phase is limited between 5 and 7 GPa.

(3) The $\alpha'(\alpha$-U) phase directly transforms to the bct phase at high pressure above 13 GPa.

The image plate technique in conjunction with synchrotron radiation studies offers higher resolution and a wide dynamic range in the study of pressure-induced phase transformation in materials. The low background, high resolution, and ability to detect crystallization and orientation effects are indeed critical to resolve the low-symmetry crystal structure induced by high pressures and high temperatures in f-electron metals and alloys.

We acknowledge the support of the Metals Program, National Science Foundation (NSF) under Grant No. DMR-9403832. We acknowledge the use of the facilities at Cornell High Energy Synchrotron Source (CHESS). We would like to thank Dr. Jagan Akella for providing the Ce sample for the experiments.

[1]A. Jayaraman and R. C. Sherwood, Phys. Rev. Lett. **12**, 22 (1964).
[2]B. Johansson, Philos. Mag. **30**, 469 (1974).
[3]J. W. Allen and R. M. Martin, Phys. Rev. Lett. **49**, 1106 (1982).
[4]K. A. Gschneidner, Jr. and L. Eyring, *Handbook on the Physics and Chemistry of Rare Earths* (North-Holland, Amsterdam, 1979), Vol. I.
[5]A. K. McMahan, J. Less-Common Met. **149**, 1 (1989).
[6]W. H. Zachariasen and F. H. Ellinger, Acta Crystallogr. A **33**, 155 (1977).
[7]S. Endo, H. Sasaki, and T. Mitsui, J. Phys. Soc. Jpn. **42**, 882 (1977).
[8]J. S. Olsen, L. Gerward, U. Benedict, and J. P. Itié, Physica **133B**, 129 (1985).
[9]Y. K. Vohra and J. Akella, Phys. Rev. Lett. **67**, 3563 (1991).
[10]G. Gu, Y. K. Vohra, U. Benedict, and J. C. Spirlet, Phys. Rev. B **50**, 2751 (1994).
[11]O. Shimomura, K. Takemura, H. Fujihisa, Y. Fujii, Y. Ohishi, T. Kikegawa, Y. Amemiya, and T. Matsushita, Rev. Sci. Instrum. **63**, 967 (1992).
[12]R. J. Nelmes and M. I. McMahon, J. Synchrotron Rad. **1**, 69 (1994).
[13]P. Vinet, J. Ferrante, J. H. Rose, and J. R. Smith, J. Geophys. Res. **92**, 9319 (1987).
[14]*High Velocity Impact Phenomenon,* edited by R. Kinslow (Academic, New York, 1970).
[15]S. N. Biswas, P. van't Klooster, and N. J. Trappeniers, Physica B **103**, 235 (1981).
[16]W. B. Holzapfel, J. Phys. Chem. Solids **55**, 711 (1994).
[17]G. Gu, Ph.D. thesis, University of Alabama at Birmingham, 1995.

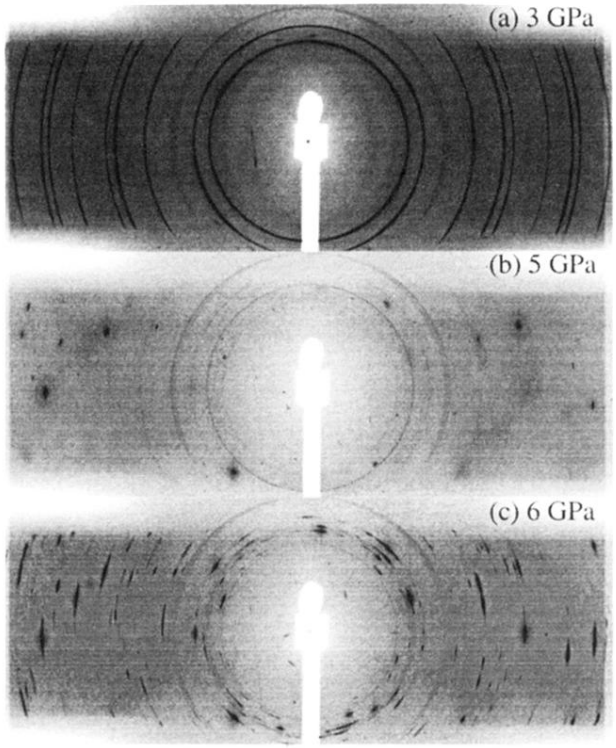

FIG. 1. X-ray-diffraction images of pure Ce metal at 3 GPa, 5 GPa, and 6 GPa, respectively. (a) At 3 GPa, the sample is in the fcc phase. (b) At 5 GPa, the large grain size of the α-U phase is indicated by only a few diffraction spots. The weak ring patterns are from the residual fcc phase. (c) The orientation effects decrease gradually at higher pressure, and rings tend to become continuous.

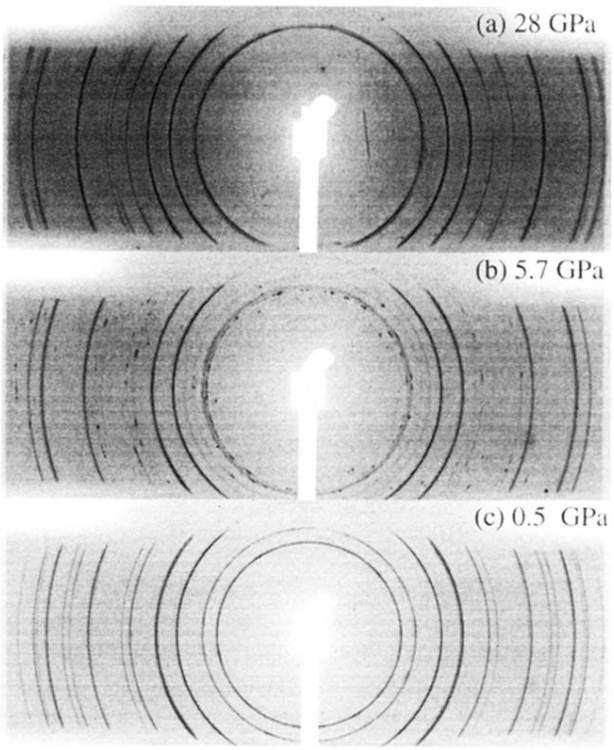

FIG. 3. X-ray-diffraction images of Ce metal mixed with the Cu pressure standard during decompression. (a) The diffraction rings are continuous and uniform in intensity for the bct phase at 28 GPa. (b) The spotty rings show the orientation effects in the α-U phase. (c) The rings become continuous and uniform again during back transformation to the fcc phase. Note that the Cu diffraction rings are always continuous through the decompression cycle.